Magnetic stripe soliton and localized stripe wave in spin-1 Bose-Einstein condensates

Li-Chen Zhao,[1,2] Xi-Wang Luo,[1] and Chuanwei Zhang[1,*]
[1]*Department of Physics, The University of Texas at Dallas, Richardson, Texas 75080, USA*
[2]*School of Physics, Northwest University, Xi'an, 710069, China*

(Received 21 March 2019; revised manuscript received 6 January 2020; accepted 5 February 2020; published 28 February 2020)

The recent experimental realization of spin-orbit coupling for ultracold atomic gases opens a new avenue for engineering solitons with internal spatial structures through tuning atomic band dispersions. However, the types of the resulting stripe solitons in a spin-1/2 Bose-Einstein condensate (BEC) have been limited to dark-dark or bright-bright with the same density profiles for different spins. Here we propose that general types of stripe solitons, including magnetic stripe solitons (e.g., dark-bright) and localized stripe waves (neither bright nor dark), could be realized in a spin-1 BEC with widely tunable band dispersions through modulating the coupling between three spin states and the linear momentum of atoms. Surprisingly, a moving magnetic stripe soliton can possess both negative and positive effective masses at different velocities, leading to a zero-mass soliton at certain velocity. Our work showcases the great potential of realizing novel types of solitons through band dispersion engineering, which may provide a new approach for exploring soliton physics in many physical branches.

DOI: 10.1103/PhysRevA.101.023621

I. INTRODUCTION

Solitons are topological defects that play significant roles in many different physical branches, such as water waves, fiber optics, and nonlinear matter waves [1–5]. Ultracold atomic superfluids, such as Bose-Einstein condensates (BECs) and degenerate Fermi gases (DFGs), provide a disorder-free and highly controllable platform for exploring soliton physics [6–17]. In particular, because solitons arise from the interplay between band dispersion and nonlinearity, tuning atomic interactions through Feshbach resonance [18] provides a tunable knob for generating various types of solitons and exploring their dynamical properties. For instance, a dark (bright) soliton has been observed in a single-component BEC with repulsive (attractive) interaction [12–14], while combinations of solitons, such as dark-dark and dark-bright solitons, have been realized in multiple-component BECs with different inter- and intracomponent interactions [15–17]. Notably, a "magnetic soliton" with a uniform total atom density has been predicted recently for a two-component BEC [19,20], where the dark soliton of one component is perfectly filled by the antidark soliton of the other component.

The recent experimental realization of spin-orbit coupling for ultracold atoms [21–31] opens a new avenue for exploring soliton physics through engineering atomic band dispersions [32–39]. In a spin-1/2 BEC, the spin-orbit coupling displays a double-well band dispersion, and the simultaneous occupation of two momentum space minima opens the possibility for generating solitons with internal spatial structures, i.e., the stripe density modulation [35–39]. However, the intrinsic Raman coupling for the realization of spin-orbit coupling mixes two spin states, which demands the same spatial density for different spins, and therefore only certain types of stripe solitons such as bright-bright or dark-dark can exist [35–39]. A natural question is whether general types of stripe solitons, such as magnetic stripe solitons (dark-bright or dark-antidark types) could be generated by tuning the band dispersion beyond that for spin-1/2 spin-orbit coupling.

In this paper, we address this important question by considering a spin-1 BEC with widely tunable band dispersion achieved by coupling three spin states $\{|\uparrow\rangle, |0\rangle, |\downarrow\rangle\}$ with the linear momentum of atoms. Our main results are the following.

(i) Both dark-bright and dark-antidark stripe solitons could exist for ferromagnetic or antiferromagnetic spin interactions. The dark and bright solitons reside at two band minima with different momenta, and the spin states $|\uparrow\rangle$ and $|\downarrow\rangle$ exhibit strong stripe density modulations on top of a soliton background.

(ii) By slightly tuning the spin interactions, a magnetic stripe soliton with a uniform total density could be generated. The dark-soliton dip in the state $|0\rangle$ is perfectly filled by the bright-soliton atoms in states $|\uparrow\rangle$ and $|\downarrow\rangle$, which exhibit an out-of-phase density modulation. More interestingly, the soliton's effective mass can possess both positive and negative values at different velocities, in contrast to solitons with a fixed sign of mass in previous literature [19,40–44].

(iii) When the spin interaction is comparable with the density interaction, a localized stripe wave for states $|\uparrow\rangle$ and $|\downarrow\rangle$, which is neither bright nor dark, could exist. Two local stripe density modulations reside on the same uniform background, but cancel each other, leading to a uniform spin-tensor density.

(iv) Such magnetic stripe solitons and localized stripe waves are stable and their stability is confirmed by numerically simulating the mean-field dynamical equations.

*chuanwei.zhang@utdallas.edu

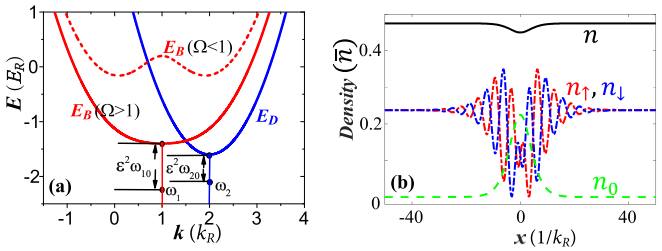

FIG. 1. (a) Single-particle band structures with detuning $\Delta = -\delta = -0.8$. The red solid (dashed) line denotes the bright band for $\Omega = 1.2$ ($\Omega = 0.4$), and the blue line denotes the dark band (independent of Ω). The $\epsilon^2\omega_{j0}$ ($j = 1, 2$) corresponds to the nonlinear energy correction induced by the soliton. (b) The spin-density distributions for a typical stripe soliton solution with antiferromagnetic interaction $g_2 > 0$. n is the total density. The parameters are $\epsilon = 0.1$, $g_2 = -0.1$, $g_0 = 1$, $\delta = 0.5$, $\omega_{10} = -42.75$, and $\omega_{20} = -47.5$.

II. SYSTEM AND METHODS

We consider the emergence of stripe solitons on the two spin states $|\uparrow\rangle$ and $|\downarrow\rangle$ through their coupling with the third state $|0\rangle$ in a spin-1 BEC. To avoid large momentum transfer between $|\uparrow\rangle$ and $|\downarrow\rangle$, while still modifying their local band dispersions, we adopt the recently proposed spin-tensor–momentum coupling for a spin-1 system [45,46], which can be realized by coupling three hyperfine ground states (denoted as $\{|\uparrow\rangle, |0\rangle, |\downarrow\rangle\}$) of alkali-metal atoms through Raman and microwave transitions [a similar scheme also applies to alkaline-earth-metal(-like) atoms]. The single-particle Hamiltonian under the basis $\{|\uparrow\rangle, |0\rangle, |\downarrow\rangle\}$ reads

$$H_0 = \left(i\partial_x + 2F_z^2\right)^2 + \Delta F_z^2 + \sqrt{2}\Omega F_x + \delta(|\uparrow\rangle\langle\downarrow| + \text{H.c.}). \quad (1)$$

Here we set $\hbar = 1$ and the recoil energy $E_R = k_R^2/2m$ and momentum k_R as energy and momentum units. F_z and F_x are spin-1 vectors, Δ is the tensor Zeeman field, Ω is the Raman coupling strength between states $|\uparrow, \downarrow\rangle$ and $|0\rangle$, and δ describes the microwave coupling between $|\uparrow\rangle$ and $|\downarrow\rangle$. The typical lower-band structure is shown in Fig. 1(a), with the low-energy dynamics characterized by two bands: the dark band $E_D(k)$ (blue line) for state $|-\rangle$; the bright band $E_B(k)$ (red lines) for the mixture of states $|+\rangle$ and $|0\rangle$, where $|\pm\rangle = \frac{1}{\sqrt{2}}(|\uparrow\rangle \pm |\downarrow\rangle)$. The dark band has a minimum at $k = 2$, while the bright band may have one or two band minima depending on the Raman coupling strength Ω.

The interaction between atoms, which is needed for generating solitons, can be described under the mean -field approximation. For the simplicity of the calculation, the spin basis $\{|+\rangle, |0\rangle, |-\rangle\}$ is used with the corresponding mean-field Gross-Pitaevskii (GP) equation (see the Appendix)

$$i\partial_t\psi_j = H_0\psi_j + (g_0\bar{n} + g_2\bar{n})n\psi_j - g_2|\psi_j|^2\psi_j + \delta_{j,0}\gamma|\psi_j|^2\psi_j, \quad (2)$$

where ψ_j is the wave function at the spin state $|j\rangle$; g_2 and $g_0 > |g_2|$ are the spin and density interaction strengths, respectively; and n is the atom density with density unit $\bar{n}$ (we set $\bar{n} = 1$ without loss of generality). The term $\delta_{j,0}\gamma|\psi_j|^2\psi_j$ in the right-hand side of Eq. (2) corresponds to the additional intracomponent interaction $\frac{\gamma}{2}|\psi_0|^4$ for the spin state $|0\rangle$, which can be realized using the Feshbach resonance [18]. Hereafter $\Delta = -\delta$ is chosen so that the bright band is symmetric around $k = 1$ to obtain simple analytic soliton solutions.

Since exact analytic soliton solutions cannot be obtained for such a spin-1 system, here we derive an approximate solution using the multiscale expansion method [35,38]. We choose an ansatz for the wave functions of the soliton:

$$\psi_{+(0)} = A_{+(0)}(x)e^{ik_1x - i\omega_1 t}, \quad w\psi_- = A_-(x)e^{ik_2x - i\omega_2 t}, \quad (3)$$

where A_+, A_0, and A_- (with $|A_j| \ll 1$) describe the spatial profiles of the soliton, k_1 and k_2 are the center momenta of the soliton, and ω_1 and ω_2 are the soliton energies. The soliton amplitudes can be expanded as $A_j = \sum_\eta \epsilon^{\eta+1}\chi_j^{(\eta)}$ using a small parameter ϵ, where $\chi_j^{(\eta)}$ are slowly varying functions (i.e., $\partial_x\chi_j^{(\eta)} \sim \epsilon\chi_j^{(\eta)}$). Substituting the ansatz (3) into Eq. (2), we obtain the soliton solution and corresponding constraints on $\chi_j^{(\eta)}$ according to the solvability conditions up to the order of $O(\epsilon^3)$. It is easy to check that the leading-order solution satisfies $\chi_+^{(0)} = -\chi_0^{(0)} \equiv U(X)$ and $\chi_-^{(0)} \equiv V(X)$, with $X = \epsilon x$.

III. DARK-BRIGHT STRIPE SOLITON

Here we focus on the case $\Omega = 1$ where the bright band has a minimum at $k = 1$ and the dispersion effects are suppressed significantly. The soliton solution is static with $k_1 = 1$ and $k_2 = 2$. The leading order in the wave function (3) yields $A_+(x) = -A_0(x) \approx \epsilon U(X)$, $A_-(x) = \epsilon V(X)$, $\omega_1 \approx E_B(1) - \epsilon^2\omega_{10}$, and $\omega_2 \approx E_D(2) - \epsilon^2\omega_{20}$, with the energy corrections $\epsilon^2\omega_{10}$ and $\epsilon^2\omega_{20}$ induced by the nonlinear interaction. For $\gamma = 0$, the mean-field equation (2) can be approximated as

$$\partial_X^2 V(X) + g_V|V(X)|^2V(X) + w_V V(X) = 0, \quad (4)$$

where the coefficients $g_V = (2g_2^2 + 3g_0g_2)/(2g_0 + g_2)$ and $w_V = 2(g_0 + g_2)\omega_{10}/(2g_0 + g_2) - \omega_{20}$. $U(X)$ can be determined through the constraint

$$|U(X)|^2 + \frac{g_0 + g_2}{2g_0 + g_2}|V(X)|^2 = \frac{-\omega_{10}}{2g_0 + g_2} > 0. \quad (5)$$

Since g_V has the same sign as g_2, the effective interaction strength $g_V < 0$ or $g_V > 0$ in Eq. (4) for ferromagnetic ($g_2 < 0$) and antiferromagnetic ($g_2 > 0$) spin interactions, respectively. For $g_V < 0$, Eqs. (4) and (5) have a dark-soliton solution,

$$V(X) = \sqrt{\frac{w_V}{-g_V}}\tanh\left[\sqrt{\frac{w_V}{2}}X\right], \quad (6)$$

in the parameter region $\frac{g_0+g_2}{g_V} \geqslant \frac{\omega_{10}}{\omega_V}$ and $w_V > 0$. The corresponding U from Eq. (5) is a bright or antidark soliton. While for $g_V > 0$,

$$V(X) = \sqrt{\frac{-2w_V}{g_V}}\,\text{sech}[\sqrt{-w_V}X] \quad (7)$$

is a bright soliton in the parameter region $\frac{g_0+g_2}{g_V} \leqslant \frac{\omega_{10}}{2\omega_V}$ and $w_V < 0$, and U is a dark soliton. Such dark-bright solutions at two band minima are different from previous bright-bright or dark-dark soliton solutions in a spin-1/2 BEC [35–37,39]. The stripe solitons for the spin states $|\uparrow\rangle$ and $|\downarrow\rangle$ are formed

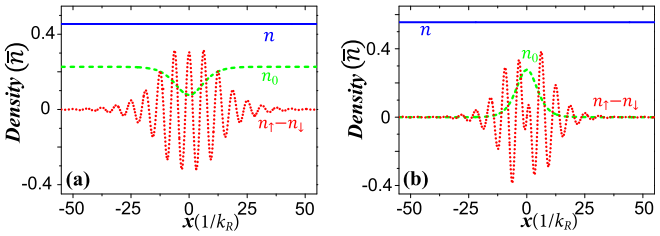

FIG. 2. (a) and (b) The spin-density distributions for the magnetic stripe soliton with $g_2 > 0$ and $g_2 < 0$, respectively. The total density is uniform, while the spin density $\mathcal{F}_z = n_\uparrow - n_\downarrow$ exhibits stripe modulation. The parameters are $g_2 = 0.1$ and $\omega_{20} = -48.5$ for panel (a) and $g_2 = -0.1$ and $\omega_{20} = -\frac{g_0}{g_0+g_2}\omega_{10}$ for panel (b). Other parameters are $\epsilon = 0.1$, $g_0 = 1$, $\gamma = 2g_2$, $\Omega = 1$, $\omega_{10} = -50$, and $\delta = 0.5$.

by the superposition of such bright-dark solitons at two band minima, leading to strong out-of-phase density modulations for two states, as shown in Fig. 1(b). The total density $n \equiv 2|U|^2 + |V|^2 = \frac{-2\omega_{10}}{2g_0+g_2} - \frac{g_2}{2g_0+g_2}|V|^2$ possesses a weak soliton profile ($\sim|V|^2$) on top of a uniform background, $\frac{-2\omega_{10}}{2g_0+g_2}$ [see Fig. 1(b)]. Similar types of solitons also exist for $\Omega > 1$ although analytic solutions are hard to obtain.

IV. MAGNETIC STRIPE SOLITONS

For typical nonlinear interactions in Eq. (2) with $\gamma = 0$, the dark soliton dip cannot be perfectly filled by the bright soliton particles, leading to a small dip for the total density. We note that it is possible to construct the magnetic stripe soliton with the uniform total density, with $\gamma \neq 0$.

For $\Omega = 1$, the soliton solution is still static and V takes the same form, Eq. (6) or Eq. (7), as that for $\gamma = 0$, except that g_V and ω_V change to $g_V = \frac{2g_2^2+3g_0g_2-g_0\gamma/2}{2g_0+g_2+\frac{\gamma}{2}}$ and $w_V = \frac{2(g_0+g_2)\omega_{10}}{2g_0+g_2+\frac{\gamma}{2}} - \omega_{20}$. Equation (5) for determining U is modified by replacing $2g_0 + g_2$ in the denominator with $2g_0 + g_2 + \gamma/2$. The total density is $n = \frac{-2\omega_{10}}{2g_0+g_2+\gamma/2} - \frac{g_2-\gamma/2}{2g_0+g_2+\gamma/2}|V|^2$, which becomes uniform when $\gamma = 2g_2$. The spin-density profiles for the magnetic stripe soliton with (anti)ferromagnetic interaction $g_2 < 0$ ($g_2 > 0$) are shown in Figs. 2(a) and 2(b). While the total density is uniform, the spin density $\mathcal{F}_z = n_\uparrow - n_\downarrow$ exists as stripe density modulation. For $g_2 < 0$, the magnetic stripe soliton may be formed either by dark and bright solitons or by dark and antidark solitons, while the latter may have a striped spin background (see the Appendix).

For $\Omega > 1$, the general soliton solution for an arbitrary γ is not easy to obtain. However, the magnetic stripe soliton with a constant total density $n = C$, which requires $\gamma = g_2(6 - \frac{4}{\Omega})$, can be obtained analytically. Such a magnetic stripe soliton for $\Omega > 1$ can have a finite velocity, with the wave functions

$$U(X,T) = \sqrt{\frac{n_v}{2}}\,\mathrm{sech}[f(X - vT)]\exp(i\delta kX), \tag{8}$$

$$V(X,T) = \sqrt{n_v}\tanh[f(X - vT)] + \frac{iv}{\sqrt{2C|g_2|}}, \tag{9}$$

for $g_2 < 0$. Here $f(X - vT) = \sqrt{|g_2|n_v}(X - vT)$, $n_v = C + \frac{v^2}{2g_2}$, and $\delta k = \frac{\Omega v}{2(\Omega-1)}$ corresponds to a small derivation of the center momentum away from the band minimum. Notice that

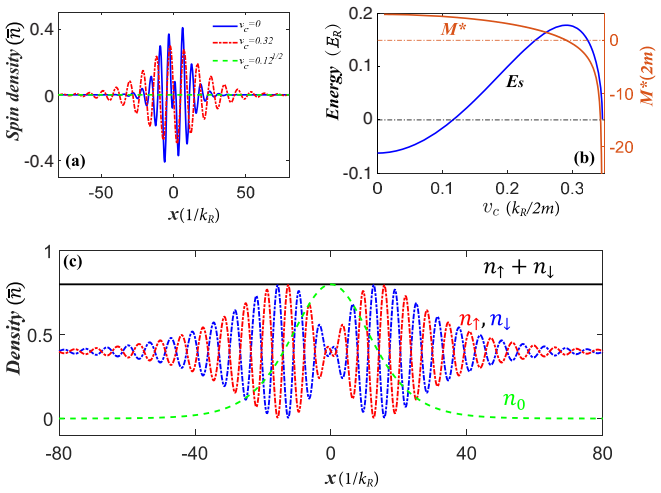

FIG. 3. (a) The moving magnetic stripe soliton profiles at different velocities. (b) The energy E_s (blue line) and the effective mass $M^* = \frac{\partial E_s}{\partial v_c^2}$ (red line) of the magnetic stripe soliton versus its velocity. Other parameters for panels (a) and (b) are $\epsilon = 0.1$, $g_2 = -0.1$, $g_0 = 1$, $\Omega = 2$, $\gamma = 4g_2$, $C = 60$, and $\delta = 1.5055$. (c) Density profiles for localized stripe waves. The spin-tensor density $\mathcal{F}_z^2 = n_\uparrow + n_\downarrow$ is a constant. The parameters are $\epsilon = 0.1$, $g_2 = -0.1$, $g_0 = 0.19$, $\Omega = 1$, $\gamma = -2g_0$, $\omega_{10} = -7.2$, $\omega_{20} = \frac{g_0}{g_0+g_2}\omega_{10}$, and $\delta = 0.5$.

the solution is valid only when Ω is not so close to 1 to ensure a small δk. $T = \epsilon^2 t$ describes the slowly varying time, and the velocity parameter $v \leqslant \sqrt{2C|g_2|}$ should be always less than the sound speed of the background. The soliton energies induced by the nonlinear interaction read $\omega_{10} = -g_0C - g_2C\frac{3\Omega-1}{2\Omega} - v^2\frac{2\Omega^2-2\Omega+1}{4\Omega(\Omega-1)}$ and $\omega_{20} = -g_0C$. Such a magnetic stripe soliton has a velocity $v_c = \epsilon v$ with respect to the static particle density background. The profile of the magnetic stripe soliton depends on its velocity: the peak value decreases while its spatial width increases with the velocity [as shown in Fig. 3(a)]. Similar soliton solutions can be obtained for $g_2 > 0$.

The moving soliton usually can be described as a quasiparticle with an effective mass and energy. The energy E_s of the soliton is defined as the difference between the grand canonical energies in the presence and absence of the soliton (with the same particle density background), while the effective mass $M^* = \frac{\partial E_s}{\partial(v_c^2)}$ [19,44] is determined accordingly. In Fig. 3(b), the energy and the effective mass of the moving stripe soliton are plotted versus its velocity. The energy increases first and then decreases as the velocity increases, while the effective mass possesses both negative and positive values and crosses zero at a velocity smaller than the sound speed. Close to the sound speed, the effective mass approaches infinity due to the velocity dependence of the dark-bright soliton profiles. These characters, especially the zero mass at a velocity less than the sound speed, are in sharp contrast to bright or dark solitons with a fixed sign of mass in previous studies [40–44]. Recently, the positive mass and negative mass of solitons in a spin-orbit coupled BEC [38], which is induced by the effective mass of a single atom (single-particle band dispersion), was discussed. The negative mass of a magnetic stripe soliton is mainly induced by nonlinearity instead of by single-particle band dispersion. Therefore, a

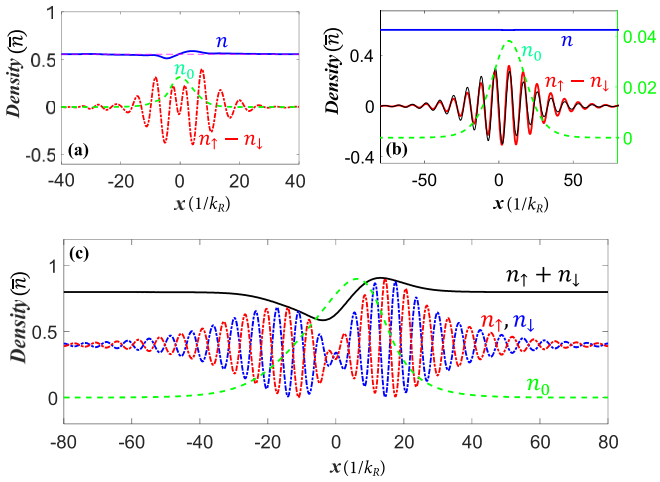

FIG. 4. (a) and (b) Numerical simulations for the magnetic stripe solitons in Figs. 2(b) and 3(b). (c) Numerical simulation for the localized stripe wave in Fig. 3(c). The evolution time is $t = 20$. The solitons are stable and the high-order corrections are negligible in panels (a) and (b) but are more significant for panel (c). The thin purple dashed line in panel (a) is the initial total density, and the thin black solid line in panel (b) is the initial stripe density modulation.

magnetic stripe soliton can admit negative mass even though the effective single-particle mass is positive, leading to very unique properties such as the infinity and zero mass at different velocities. We note that similar tunable inertial masses of atomic Josephson vortices and related solitary waves can also be achieved through an adjustable linear coupling between the two components in a BEC [47]. These striking inertial mass properties could inspire more discussions on the dispersion relation of quasiparticle nonlinear waves.

V. LOCALIZED STRIPE WAVE

In stripe solitons discussed in either spin-1/2 BEC [35–39] or above magnetic stripe solitons, the striped density modulation resides on a bright or dark soliton background. Here such a density background is given by $|U|^2 + |V|^2$, which can be tuned to be uniform by the spin-dependent interaction γ; therefore the stripe soliton for states $|\uparrow\rangle$ and $|\downarrow\rangle$ is neither bright nor dark, but rather a localized stripe wave. For instance, when $\Omega = 1$ and $\gamma = -2g_0$, the spin-tensor density $\mathcal{F}_z^2 = n_\uparrow + n_\downarrow$ becomes uniform. For $g_2 > 0$ ($g_2 < 0$), the localized stripe waves for states $|\uparrow\rangle$ and $|\downarrow\rangle$ exist for $\frac{2w_V}{g_V} \leqslant \frac{-\omega_{10}}{g_0+g_2}$ ($\frac{w_V}{|g_V|} = \frac{-\omega_{10}}{g_0+g_2}$), while state $|0\rangle$ admits a dark (bright) soliton profile, as shown in Fig. 3(c).

VI. STABILITY OF SOLITONS

To check the stability of these stripe solitons obtained from the multiscale expansion method, we numerically simulate the time evolution dynamics of the obtained solitons using the GP equation (2) with the analytic soliton solutions as the initial states. As an example, we consider the magnetic stripe solitons for ferromagnetic interaction ($g_2 < 0$). Both static [$\Omega = 1$ in Fig. 2(b)] and moving [$\Omega > 1$ and $v_c = 0.32$ in Fig. 3(a)] solitons are found to be stable [see Figs. 4(a) and 4(b)]. We notice that higher-order terms in the solution may induce slight modulation of the soliton profile, which is typically of the order of ϵ^2. In addition, a nonzero γ breaks the balance between states $|+\rangle$ and $|0\rangle$, leading to small atom transitions between them. However, as long as γ is weak compared with the density interaction g_0, such transitions hardly affect the stability of the soliton and the uniformity of the total density.

The localized stripe wave requires a γ that is comparable with g_0, yielding a strong coupling between states $|+\rangle$ and $|0\rangle$. Nevertheless, we find that stable solitons can still exist when both γ and g_0 are weak compared with the recoil energy. In Fig. 4(c), we show our numerical result with density interaction $g_0 = 1.9|g_2|$, $g_2 < 0$, and $\gamma = -2g_0$. Although the localized stripe wave is stable, the spin background $|U|^2 + |V|^2$ is no longer uniform, but exhibits a soliton profile due to the nonzero γ (which is comparable with g_0). The numerical simulations of the dark-bright stripe solitons with $\gamma = 0$ are shown in the Appendix and are in good agreement with Fig. 1(b) thanks to the absence of transitions between states $|+\rangle$ and $|0\rangle$.

VII. DISCUSSION AND CONCLUSION

The spin interaction g_2 (either >0 or <0) of alkali-metal atoms is usually much smaller than the density interaction g_0 [48–50]. The intracomponent interaction strength γ for state $|0\rangle$ can be realized by using an additional Feshbach resonance [18]. In our simulation of the magnetic stripe soliton, we consider $g_2 = \pm 0.1 g_0$, and as we increase (decrease) $|g_2|$, the soliton properties will not be affected, except that its size may decrease (increase) slightly. Different from the ground-state stripe phase, the stripe solitons can exist in a large parameter region and the choice of Ω and Δ is very flexible. This is because the solitons are metastable states and we can have solutions even when the detuning between two (bright and dark) band minima are much larger than g_2. We focus our study in the $\Omega \geqslant 1$ region. For $\Omega < 1$, the bright band has two band minima around $k = 1$, and there still exist magnetic stripe soliton solutions with k_1 located at one of two band minima (see the Appendix). In experiments, the soliton may be imprinted at the center of the BEC cloud using light-induced spatial-dependent potential, and observed after some evolution time [6–8].

In summary, we demonstrate alternative types of stripe solitons, such as magnetic stripe solitons and localized stripe waves, can be engineered by tuning the band dispersion in a spin-1 BEC with spin-orbit coupling. These solitons are quite different from the solitons in the spin-orbit-coupled BEC [34–38], which further enrich the soliton family in the BEC and many other nonlinear systems and may be used for both fundamental studies (e.g., spin-orbital coupling, nonlinear effects, quantum fluctuations [51–53], modulational instability [54], and quantum entanglement [55]) and realistic applications (e.g., atomic soliton laser). The striking effective mass characters of these solitons may shed light on the study of particle physics [56,57]. While many interesting problems, such as the generalization of magnetic stripe solitons to higher dimensions [33,58–60], remain to be explored, our work clearly showcases the power of soliton generation through band dispersion engineering, which may

provide a new approach for exploring soliton physics in many physical branches.

ACKNOWLEDGMENTS

L.-C.Z. is supported by the National Natural Science Foundation of China (Contract No. 11775176), the Major Basic Research Program of the Natural Science of Shaanxi Province (Grant No. 2018KJXX-094), and the China Scholarship Council. X.-W.L. and C.Z. are supported by the Air Force Office of Scientific Research (Grant No. FA9550-16-1-0387), the National Science Foundation (Grant No. PHY-1806227), and the Army Research Office (Grant No. W911NF-17-1-0128).

APPENDIX

In this Appendix, we derive the nonlinear Schrödinger equation of the spin-1 system and give the magnetic stripe soliton solutions in other parameter regions not shown in the main text.

1. Nonlinear Schrödinger equation

In the lab frame, the second-quantization Hamiltonian can be written as

$$\mathcal{H} = \int dx \Psi^\dagger H_0 \Psi + \int dx \frac{g_0}{2}(\Psi^\dagger\Psi)^2 + \frac{\gamma}{2}(\psi_0^\dagger\psi_0)^2 + \frac{g_2}{2}(\Psi^\dagger \mathbf{F}\Psi)^2,$$

with spin operator $\mathbf{F} = (F_x, F_y, F_z)$ and atom field $\Psi = (\psi_\uparrow, \psi_0, \psi_\downarrow)$. The nonlinear Schrödinger equation can be obtained by

$$i\partial_t \Psi = [\Psi, \mathcal{H}].$$

In the quasimomentum frame, we have [45]

$$i\partial_t \psi_j = H_0\psi_j + (g_0\bar{n} + g_2\bar{n})n\psi_j - g_2|\psi_j|^2\psi_j + \delta_{j,0}\gamma|\psi_j|^2\psi_j + g_2\psi_j^* Q_j(x),$$

where $j = \pm, 0$ and $Q_+(x) = \psi_-^2 + \psi_0^2 e^{i4x}$, $Q_-(x) = \psi_+^2 - \psi_0^2 e^{i4x}$, and $Q_0(x) = (\psi_+^2 - \psi_-^2)e^{-i4x}$. We are interested in the solutions with momenta centering at the band minima, while the last term involves couplings with higher momenta far away from the band minima, therefore its effect is negligible and can be omitted. This is also confirmed by our numerical simulation in Fig. 5, where the last term only induces tiny and fast spatial modulations without affecting the soliton profile.

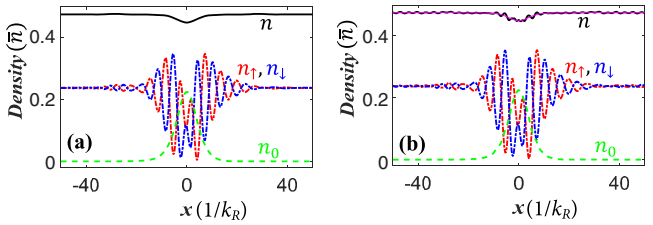

FIG. 5. (a) and (b) Numerical results of the soliton profiles at $t = 20$ without and with the Q_j terms. The parameters are the same as those in Fig. 1(b) in the main text. The thin purple line at the top of panel (b) is the total density without the Q_j term [same as the black line in panel (a)].

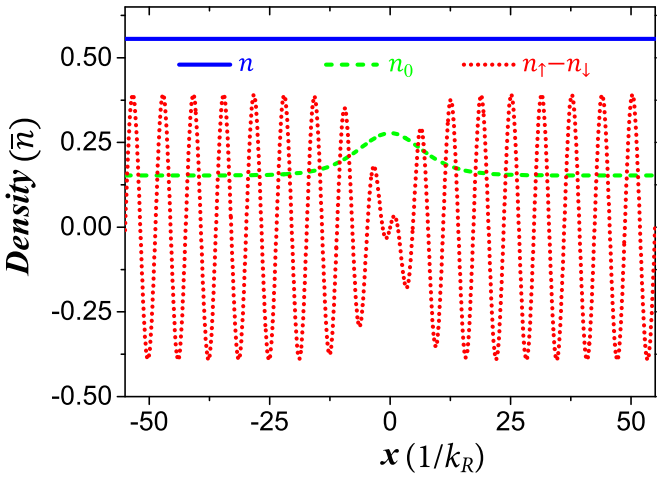

FIG. 6. The spatial profiles of dark-antidark magnetic stripe solitons. The parameters are $\epsilon = 0.1$, $g_2 = -0.1$, $g_0 = 1$, $\omega_{10} = -50$, $\omega_{20} = -52.5$, and $\delta = 0.5$.

2. Dark-antidark magnetic stripe solitons

In the main text, we have focused on magnetic stripe solitons formed by dark and bright solitons, which admit spin-balanced background. However, at $\Omega = 1$, the spin background can be imbalanced if it is formed by dark and antidark solitons. Such dark and antidark solitons can exist for ferromagnetic interactions $g_2 < 0$ with the proper choice of parameters (i.e., ω_{10} and ω_{20}), as shown in Fig. 6 (its stability is confirmed numerically). The soliton resides on a striped spin background, which is different from the stripe magnetic solitons with a zero spin background (as shown in Fig. 2 of the main text).

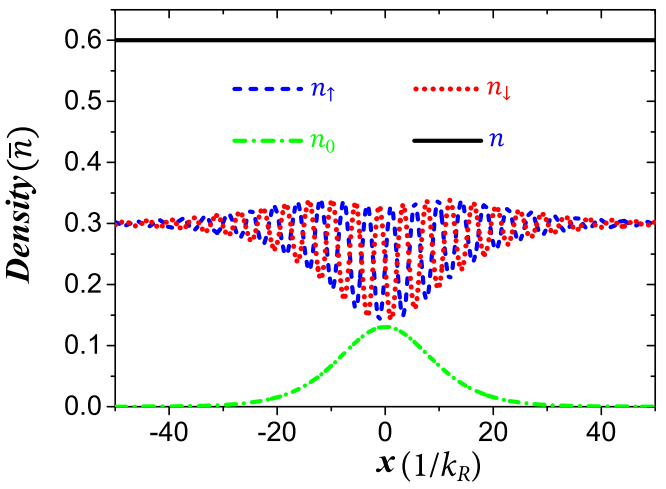

FIG. 7. The magnetic stripe soliton for $\Omega < 1$ and $g_2 < 0$. A numerical test shows that it is stable. The center momentum is $k_1 = 1 - \sqrt{1-\Omega^2}$, and the additional spin-dependent modulation coefficient is $\gamma = \frac{2g_2(3\Omega^2-4)(\Omega^2+2\sqrt{1-\Omega^2}-2)}{\Omega^4}$. Other parameters are $\epsilon = 0.1$, $g_2 = -0.1$, $g_0 = 1$, $\Omega = 2/3$, $n_1 = 60$, $\omega_{10} = 0$, $\omega_{20} = 0$, $\delta = 4/18$, and $v = 3$.

3. Magnetic stripe solitons for Ω < 1

For $\Omega < 1$, the bright band has two minima at $k = 1 \pm \sqrt{1-\Omega^2}$, thus we expect to find stable stripe solitons by choosing the center momentum as $k_1 = 1 \pm \sqrt{1-\Omega^2}$. Magnetic stripe solitons with a uniform total density require $\gamma = \frac{2g_2(3\Omega^2-4)(\Omega^2+2\sqrt{1-\Omega^2}-2)}{\Omega^4}$. As an example, we present a stripe soliton solution for $g_2 < 0$ and $k_1 = 1 - \sqrt{1-\Omega^2}$, while similar soliton solutions can be obtained in other parameter regimes. The stripe-magnetic-soliton wave functions are $\psi_\uparrow \approx \frac{1}{\sqrt{2}}\epsilon[\frac{\sqrt{1-\Omega^2}-1}{\Omega}U(X,T)e^{ik_1x-i\omega_1t} + V(X,T)e^{ik_2x-i\omega_2t}]$, $\psi_0 \approx \epsilon U(X,T)e^{ik_1x-i\omega_1t}$, and $\psi_\downarrow \approx \frac{1}{\sqrt{2}}\epsilon[\frac{\sqrt{1-\Omega^2}-1}{\Omega}U(X,T)e^{ik_1x-i\omega_1t} - V(X,T)e^{ik_2x-i\omega_2t}]$, where $U(X,T)$ and $V(X,T)$ are

$$U(X,T) = \sqrt{\frac{p}{\gamma_r}}\,\mathrm{sech}\left[\sqrt{\frac{p}{2}}(X-vT)\right]\exp\left(-\frac{iT_1[n_1(g_0+g_2)+\omega_{10}]}{1-\Omega^2} + \frac{ipT_1}{2} - \frac{1}{4}iT_1v_1^2 + \frac{iv_1X}{2}\right), \tag{A1}$$

$$V(X,T) = \sqrt{n_1}\left\{\sqrt{1-\frac{v^2}{2(-g_2)n_1}}\tanh\left[\sqrt{\frac{1}{2}(-g_2)n_1}\sqrt{1-\frac{v^2}{2(-g_2)n_1}}(X-vT)\right] + \frac{iv}{\sqrt{2(-g_2)n_1}}\right\}\exp[i\phi], \tag{A2}$$

with $\gamma_r = \frac{\frac{g_2(2-\Omega^2)(1-\sqrt{1-\Omega^2})}{\Omega^2} - \frac{1}{2}\gamma(\sqrt{1-\Omega^2}+1)}{1-\Omega^2}$, $p = \frac{1}{2}(-2g_2n_1 - v^2)$, $v_1 = \frac{v}{1-\Omega^2}$, $T_1 = (1-\Omega^2)T$, and $\phi = g_2n_1T - n_1(g_0+g_2)T + \omega_{20}T$.

Figure 7 shows the typical density (spin) profiles of such solitons. The soliton is confirmed to be stable in the GP equation simulation, although higher-order terms in the solution may induce minor distortion.

[1] P. G. Drazin and R. S. Johnson, *Solitons: An Introduction* (Cambridge University, Cambridge, England, 2002).

[2] L. A. Dickey, *Soliton Equations and Hamiltonian Systems* (World Scientific, New York, 2003).

[3] Y. S. Kivshar and G. P. Agrawal, *Optical Solitons* (Academic, San Diego, 2003).

[4] P. G. Kevrekidis, D. J. Frantzeskakis, and R. Carretero-Gonz ález, *Emergent Nonlinear Phenomena in Bose-Einstein Condensates: Theory and Experiment* (Springer, Heidelberg, 2007).

[5] A. C. Scott, F. Y. F. Chu, and D. W. McLaughlin, The soliton: A new concept in applied science, Proc. IEEE **61**, 1443 (1973).

[6] S. Burger, K. Bongs, S. Dettmer, W. Ertmer, K. Sengstock, A. Sanpera, G. V. Shlyapnikov, and M. Lewenstein, Dark Solitons in Bose-Einstein Condensates, Phys. Rev. Lett. **83**, 5198 (1999).

[7] J. Denschlag *et al.*, Generating solitons by phase engineering of a Bose-Einstein condensate, Science **287**, 97 (2000).

[8] B. P. Anderson, P. C. Haljan, C. A. Regal, D. L. Feder, L. A. Collins, C. W. Clark, and E. A. Cornell, Watching Dark Solitons Decay into Vortex Rings in a Bose-Einstein Condensate, Phys. Rev. Lett. **86**, 2926 (2001).

[9] T. Yefsah, Ariel T. Sommer, M. J. H. Ku, L. W. Cheuk, W. Ji, Waseem S. Bakr, and M. W. Zwierlein, Heavy solitons in a fermionic superfluid, Nature (London) **499**, 426 (2013).

[10] N. Meyer, H. Proud, M. Perea-Ortiz, C. O'Neale, M. Baumert, M. Holynski, J. Kronjäger, G. Barontini, and K. Bongs, Observation of Two-Dimensional Localized Jones-Roberts Solitons in Bose-Einstein Condensates, Phys. Rev. Lett. **119**, 150403 (2017).

[11] T. M. Berano, V. Gokroo, M. A. Khamehchi, J. D. Abroise, D. J. Frantzeskakis, P. Engles, and P. G. Kevrekidis, Three-Component Soliton States in Spinor $F = 1$ Bose-Einstein Condensates, Phys. Rev. Lett. **120**, 063202 (2018).

[12] J. H. V. Nguyen, P. Dyke, D. Luo, B. A. Malomed, and R. G. Hulet, Collisions of matter-wave solitons, Nat. Phys. **10**, 918 (2014).

[13] K. E. Strecker, G. B. Partridge, A. G. Truscott, and R. G. Hulet, Formation and propagation of matter-wave soliton trains, Nature (London) **417**, 150 (2002).

[14] L. Khaykovich, F. Schreck, G. Ferrari, T. Bourdel, J. Cubizolles, L. D. Carr, Y. Castin, and C. Salomon, Formation of a matter-wave bright soliton, Science **296**, 1290 (2002).

[15] C. Hamner, J. J. Chang, P. Engels, and M. A. Hoefer, Generation of Dark-Bright Soliton Trains in Superfluid-Superfluid Counterflow, Phys. Rev. Lett. **106**, 065302 (2011).

[16] C. Becker, S. Stellmer, P. S. Panahi *et al.*, Oscillations and interactions of dark and dark-bright solitons in Bose-Einstein condensates, Nat. Phys. **4**, 496 (2008).

[17] M. A. Hoefer, J. J. Chang, C. Hamner, and P. Engels, Dark-dark solitons and modulational instability in miscible two-component Bose-Einstein condensates, Phys. Rev. A **84**, 041605(R) (2011).

[18] C. Chin, R. Grimm, P. Julienne, and E. Tiesinga, Feshbach resonances in ultracold gases, Rev. Mod. Phys. **82**, 1225 (2010).

[19] C. Qu, L. P. Pitaevskii, and S. Stringari, Magnetic Solitons in a Binary Bose-Einstein Condensate, Phys. Rev. Lett. **116**, 160402 (2016).

[20] C. Qu, M. Tylutki, S. Stringari, and L. P. Pitaevskii, Magnetic solitons in Rabi-coupled Bose-Einstein condensates, Phys. Rev. A **95**, 033614 (2017).

[21] Y.-J. Lin, K. Jiménez-García, and I. B. Spielman, Spin-orbit-coupled Bose-Einstein condensates, Nature (London) **471**, 83 (2011).

[22] J.-Y. Zhang *et al.*, Collective Dipole Oscillations of a Spin-Orbit Coupled Bose-Einstein Condensate, Phys. Rev. Lett. **109**, 115301 (2012).

[23] C. Qu, C. Hamner, M. Gong, C. Zhang, and P. Engels, Observation of *Zitterbewegung* in a spin-orbit-coupled Bose-Einstein condensate, Phys. Rev. A **88**, 021604 (2013).

[24] A. Olson, S. Wang, R. Niffenegger, C. Li, C. Greene, and Y. Chen, Tunable Landau-Zener transitions in a spin-orbit-coupled Bose-Einstein condensate, Phys. Rev. A **90**, 013616 (2014).

[25] P. Wang *et al.*, Spin-Orbit Coupled Degenerate Fermi Gases, Phys. Rev. Lett. **109**, 095301 (2012).

[26] L. W. Cheuk *et al.*, Spin-Injection Spectroscopy of a Spin-Orbit Coupled Fermi Gas, Phys. Rev. Lett. **109**, 095302 (2012).

[27] R. A. Williams *et al.*, Raman-Induced Interactions in a Single-Component Fermi Gas Near an *s*-Wave Feshbach Resonance, Phys. Rev. Lett. **111**, 095301 (2013).

[28] L. Huang *et al.*, Experimental realization of two-dimensional synthetic spin-orbit coupling in ultracold Fermi gases, Nat. Phys. **12**, 540 (2016).

[29] Z. Wu *et al.*, Realization of two-dimensional spin-orbit coupling for Bose-Einstein condensates, Science **354**, 83 (2016).

[30] D. Campbell, R. Price, A. Putra, A. Valdés-Curiel, D. Trypogeorgos, and I. B. Spielman, Magnetic phases of spin-1 spin-orbit-coupled Bose gases, Nat. Commun. **7**, 10897 (2016).

[31] X. Luo *et al.*, Tunable atomic spin-orbit coupling synthesized with a modulating gradient magnetic field, Sci. Rep. **6**, 18983 (2016).

[32] O. Fialko, J. Brand, and U. Zülicke, Soliton magnetization dynamics in spin-orbit-coupled Bose-Einstein condensates, Phys. Rev. A **85**, 051605(R) (2012).

[33] Y.-C. Zhang, Z.-W. Zhou, B. A. Malomed, and H. Pu, Stable Solitons in Three-Dimensional Free Space without the Ground State: Self-Trapped Bose-Einstein Condensates with Spin-Orbit Coupling, Phys. Rev. Lett. **115**, 253902 (2015).

[34] Y. V. Kartashov and V. V. Konotop, Solitons in Bose-Einstein Condensates with Helicoidal Spin-Orbit Coupling, Phys. Rev. Lett. **118**, 190401 (2017).

[35] V. Achilleos, D. J. Frantzeskakis, P. G. Kevrekidis, and D. E. Pelinovsky, Matter-Wave Bright Solitons in Spin-Orbit Coupled Bose-Einstein Condensates, Phys. Rev. Lett. **110**, 264101 (2013).

[36] Y. Xu, Y. Zhang, and B. Wu, Bright solitons in spin-orbit-coupled Bose-Einstein condensates, Phys. Rev. A **87**, 013614 (2013).

[37] V. Achilleos, D. J. Frantzeskakis, and P. G. Kevrekidis, Beating dark-dark solitons and *Zitterbewegung* in spin-orbit-coupled Bose-Einstein condensates, Phys. Rev. A **89**, 033636 (2014).

[38] V. Achilleos, D. J. Frantzeskakis, P. G. Kevrekidis, P. Schmelcher, and J. Stockhofe, Positive and negative mass solitons in spin-orbit coupled Bose-Einstein condensates, Rom. Rep. Phys. **67**, 235 (2015).

[39] Y. Xu, Y. Zhang, and C. Zhang, Bright solitons in a two-dimensional spin-orbit-coupled dipolar Bose-Einstein condensate, Phys. Rev. A **92**, 013633 (2015).

[40] Th. Busch and J. R. Anglin, Motion of Dark Solitons in Trapped Bose-Einstein Condensates, Phys. Rev. Lett. **84**, 2298 (2000).

[41] Th. Busch and J. R. Anglin, Dark-Bright Solitons in Inhomogeneous Bose-Einstein Condensates, Phys. Rev. Lett. **87**, 010401 (2001).

[42] B. Eiermann, Th. Anker, M. Albiez, M. Taglieber, P. Treutlein, K.-P. Marzlin, and M. K. Oberthaler, Bright Bose-Einstein Gap Solitons of Atoms with Repulsive Interaction, Phys. Rev. Lett. **92**, 230401 (2004).

[43] V. V. Konotop and L. Pitaevskii, Landau Dynamics of a Grey Soliton in a Trapped Condensate, Phys. Rev. Lett. **93**, 240403 (2004).

[44] R. G. Scott, F. Dalfovo, L. P. Pitaevskii, and S. Stringari, Dynamics of Dark Solitons in a Trapped Superfluid Fermi Gas, Phys. Rev. Lett. **106**, 185301 (2011).

[45] X.-W. Luo, K. Sun, and C. Zhang, Spin-Tensor–Momentum-Coupled Bose-Einstein Condensates, Phys. Rev. Lett. **119**, 193001 (2017).

[46] X.-W. Luo and C. Zhang, Tunable spin-orbit coupling and magnetic superstripe phase in a Bose-Einstein condensate, Phys. Rev. A **100**, 063606 (2019).

[47] S. S. Shamailov and J. Brand, Quasiparticles of widely tuneable inertial mass: The dispersion relation of atomic Josephson vortices and related solitary waves, SciPost Phys. **4**, 018 (2018).

[48] T. L. Ho, Spinor Bose Condensates in Optical Traps, Phys. Rev. Lett. **81**, 742 (1998).

[49] T. Ohmi and K. Machida, Bose-Einstein condensation with internal degrees of freedom in alkali atom gases, J. Phys. Soc. Jpn. **67**, 1822 (1998).

[50] D. M. Stamper-Kurn and M. Ueda, Spinor Bose gases: Symmetries, magnetism, and quantum dynamics, Rev. Mod. Phys. **85**, 1191 (2013).

[51] H. Kadau, M. Schmitt, M. Wenzel, C. Wink, T. Maier, I. Ferrier-Barbut, and T. Pfau, Observing the Rosensweig instability of a quantum ferrofluid, Nature (London) **530**, 194 (2016).

[52] P. Cheiney, C. R. Cabrera, J. Sanz, B. Naylor, L. Tanzi, and L. Tarruell, Bright Soliton to Quantum Droplet Transition in a Mixture of Bose-Einstein Condensates, Phys. Rev. Lett. **120**, 135301 (2018).

[53] N. B. Jørgensen, G. M. Bruun, and J. J. Arlt, Dilute Fluid Governed by Quantum Fluctuations, Phys. Rev. Lett. **121**, 173403 (2018).

[54] J. H. V. Nguyen, D. Luo, and R. G. Hulet, Formation of matter-wave soliton trains by modulational instability, Science **356**, 422 (2017).

[55] B. Gertjerenken, T. P. Billam, C. L. Blackley, C. R. Le Sueur, L. Khaykovich, S. L. Cornish, and C. Weiss, Generating Mesoscopic Bell States via Collisions of Distinguishable Quantum Bright Solitons, Phys. Rev. Lett. **111**, 100406 (2013).

[56] C. Rebbi and G. Soliani, *Solitons and Particles* (World Scientific, Singapore, 1984).

[57] Y. Xu, L. Mao, B. Wu, and C. Zhang, Dark Solitons with Majorana Fermions in Spin-Orbit-Coupled Fermi Gases, Phys. Rev. Lett. **113**, 130404 (2014).

[58] S. Gautam and S. K. Adhikari, Three-dimensional vortex-bright solitons in a spin-orbit-coupled spin-1 condensate, Phys. Rev. A **97**, 013629 (2018).

[59] A. Gallemí, L. P. Pitaevskii, S. Stringari, and A. Recati, Magnetic defects in an imbalanced mixture of two Bose-Einstein condensates, Phys. Rev. A **97**, 063615 (2018).

[60] K. J. H. Law, P. G. Kevrekidis, and L. S. Tuckerman, Stable Vortex–Bright-Soliton Structures in Two-Component Bose-Einstein Condensates, Phys. Rev. Lett. **105**, 160405 (2010).